Disruption of Adenosine 2A Receptor Exacerbates NAFLD through Increasing Inflammatory Responses and SREBP1c Activity

Yuli Cai[1,2*], Honggui Li[1*], Mengyang Liu[1*], Ya Pei[1], Juan Zheng[1,3], Jing Zhou[1], Xianjun Luo[1], Wenya Huang[1], Linqiang Ma[1,4,5], Qiuhua Yang[6,7], Shaodong Guo[1], Xiaoqiu Xiao[4,5], Qifu Li[4], Tianshu Zeng[3], Fanyin Meng[8,9], Heather Francis[8,9], Shannon Glaser[8,9], Lulu Chen[3], Yuqing Huo[6,7], Gianfranco Alpini[8,9†], and Chaodong Wu[1†]

[1] Department of Nutrition and Food Science, Texas A&M University, College Station, TX 77843, USA; [2]Department of Endocrinology, Renmin Hospital, Wuhan University, Wuhan, Hubei 430060, China; [3]Department of Endocrinology, Union Hospital, Tongji College of Medicine, Huazhong University of Science and Technology, Wuhan, Hubei 430022, China; [4] Department of Endocrinology and [5] the Laboratory of Lipid & Glucose Metabolism, the First Affiliated Hospital of Chongqing Medical University, Chongqing 400016, China; [6]Vascular Biology Center, Department of Cellular Biology and Anatomy, Medical College of Georgia, Augusta University, Augusta, GA 30912, USA; [7] Drug Discovery Center, Key Laboratory of Chemical Genomics, Peking University Shenzhen Graduate School, Shenzhen 518055, China; [8] Research, Central Texas Veterans Health Care System and [9] Department of Medical Physiology, Texas A&M University College of Medicine, Temple, TX 76504, USA.

This material is the result of work partly supported by resources at the Central Texas Veterans Health Care System. The views expressed in this article are those of the authors and do not necessarily represent the views of the Department of Veterans Affairs.

*, equal contribution;

† Contact information

This article has been accepted for publication and undergone full peer review but has not been through the copyediting, typesetting, pagination and proofreading process which may lead to differences between this version and the Version of Record. Please cite this article as doi: 10.1002/hep.29777

Chaodong Wu, MD, PhD, College Station, TX 77843, Fax: 979 458 3129, Email: cdwu@tamu.edu; or Gianfranco Alpini, PhD, Temple, TX 76504, E-mail: galpini@tamu.edu; Tel: 254 743 1041

ABSTRACT

Adenosine 2A receptor ($A_{2A}R$) exerts protective roles in endotoxin- and/or ischemia-induced tissue damages. However, the role for $A_{2A}R$ in non-alcoholic fatty liver disease (NAFLD) remains largely unknown. We sought to examine the effects of global and/or myeloid cell-specific $A_{2A}R$ disruption on the aspects of obesity-associated NAFLD and to elucidate the underlying mechanisms. Global and/or myeloid cell-specific $A_{2A}R$-disrupted mice, as well as control mice were fed a high-fat diet (HFD) to induce NAFLD. Also, bone marrow-derived macrophages and primary mouse hepatocytes were examined for inflammatory and metabolic responses. Upon feeding an HFD, both global $A_{2A}R$-disrupted mice and myeloid cell-specific $A_{2A}R$-defcient mice revealed increased severity of HFD-induced hepatic steatosis and inflammation compared with their respective control mice. In *in vitro* experiments, $A_{2A}R$-deficient macrophages exhibited increased proinflammatory responses, and enhanced fat deposition of wild-type primary hepatocytes in macrophage-hepatocyte co-cultures. In primary hepatocytes, $A_{2A}R$ deficiency increased the proinflammatory responses and enhanced the effect of palmitate on stimulating fat deposition. Moreover, $A_{2A}R$ deficiency significantly increased sterol regulatory element-binding protein 1c (SREBP1c) abundance in livers of fasted mice and in hepatocytes upon nutrient deprivation. In the absence of $A_{2A}R$, SREBP1c transcription activity was significantly increased in mouse hepatocytes. Taken together, these results demonstrate that disruption of $A_{2A}R$ in both macrophage and hepatocytes accounts for increased severity of NAFLD, likely through increasing inflammation and through elevating lipogenic events due to stimulation of SREBP1c expression and transcription activity.

Key words: Adenosine 2A receptor, non-alcoholic fatty liver disease, obesity, inflammation, sterol regulatory element-binding protein 1c

Abbreviations

ACC1, acetyl-CoA carboxylase 1
$A_{2A}R$, adenosine 2A receptor
ALD, alcoholic fatty liver disease
AMPK, AMP-activated protein kinase
BMDM, bone marrow-derived macrophages
BSA, bovine serum albumin
CD, chow diet,
ChIP, chromatin immunoprecipitation
ChREBP, carbohydrate-responsive element-binding protein
CPT1a, carnitine palmitoyltransferase 1a
DMEM, Dulbecco's modified Eagle's medium
FAS, fatty acid synthase
FBS, fetal bovine serum
GAPDH, glyceraldehyde 3-phosphate dehydrogenase
GTT, glucose tolerance test
H&E, hematoxylin and eosin
HFD, high-fat diet
LFD, low-fat diet
IL-1β, interleukin 1β
IL-6, interleukin 6
ITT, insulin tolerance test
LPS, lipopolysaccharide
JNK, c-Jun N-terminal kinases
MCD, methionine- and choline-deficient diet
NAFLD, non-alcoholic fatty liver disease
NASH, non-alcoholic steatohepatitis
NFκB, nuclear factor kappa B
PBS, phosphate-buffered saline
P-Akt, phosphorylated Akt
Pp65, phosphorylated p65 subunit of NFκB
Pp46, phosphorylated JNK1 (p46)
RQ, respiratory quotient
SREBP1c, sterol regulatory element-binding protein 1c
TG, triglycerides
TNFα, tumor necrosis factor α
WAT, white adipose tissue

INTRODUCTION

Hepatic steatosis is a hallmark of non-alcoholic fatty liver disease (NAFLD) (1, 2). When the liver develops overt inflammatory damage, simple steatosis progresses to non-alcoholic steatohepatitis (NASH) (2, 3). The latter is the advanced form of NAFLD and is considered as a leading causal factor of cirrhosis and hepatocellular carcinoma (4, 5). In addition, NAFLD critically contributes to the development of dyslipidemia and significantly increases the incidence of atherogenic cardiovascular diseases (6), thereby serving as a key component of metabolic syndrome (7).

Numerous studies from both human subjects and rodent models demonstrate that obesity significantly increases the incidence of NAFLD (8-10). Accordingly, obesity-associated inflammation is accepted as a critical factor that initiates or exacerbates NAFLD. For instance, inflammation can cause hepatic insulin resistance, which, in turn elevates hepatic steatosis, at least in part, through increasing the expression of genes for lipogenic enzymes such as acetyl-CoA carboxylase 1 (ACC1) and fatty acid synthase (FAS), and decreasing the expression of genes for fatty acid oxidation including carnitine palmitoyltransferase 1a (CPT1a) (11-13). In addition, proinflammatory mediators, e.g., cytokines, can exert direct effects on hepatocytes to increase lipogenic events (14), and act on both hepatocytes and liver macrophages/Kupffer cells to accelerate liver inflammation. This exemplifies how inflammation serves as "a second hit" to drive the progression of simple steatosis to NASH. However, exactly how inflammation is regulated in the context of NAFLD pathophysiology remains largely unclear.

Adenosine receptors, including A_1, A_{2A}, A_{2B} and A_3, belong to the superfamily of G-protein-coupled receptors, and mediate various physiological functions of adenosine (15). Among the four adenosine receptors, $A_{2A}R$ displays powerful anti-inflammatory effects in immune cells such as macrophages and neutrophils (15, 16). Several studies in animal models have indicated that $A_{2A}R$ deficiency exacerbates concanavalin A- or endotoxin-induced liver damage, which is attributable to prolonged and enhanced expression of proinflammatory cytokines including tumor necrosis factor alpha (TNFα) and interleukin-6 (IL-6) (17). Also, there is a study showing that $A_{2A}R$ deficiency exacerbates the severity of aspects of alcoholic fatty liver disease (ALD) in mice (18). Additionally, $A_{2A}R$ activation displays beneficial effects on aspects of NASH in rodents (19, 20), which is largely mediated through the anti-inflammatory effect of $A_{2A}R$. In contrast, treatment of mice with an $A_{2A}R$ antagonist increased the severity of CCl_4-induced liver fibrosis; although the same treatment reversed the effect of ethanol on exacerbating CCl_4-induced liver fibrosis (21). Collectively, these findings suggest that $A_{2A}R$ has a protective role in liver damage. However, whether and how $A_{2A}R$ coordinates hepatocyte and macrophage metabolic and/or inflammatory responses to alter NAFLD development and progression remains poorly understood. It is also not clear whether and how $A_{2A}R$ regulates hepatocyte lipogenic events, whose increase is of particular importance in the pathogenesis of hepatic steatosis. The present study aimed to examine how global and/or myeloid cell-specific $A_{2A}R$ disruption influences NAFLD aspects in mice and provides the primary evidence to support a protective role for the $A_{2A}R$ in both macrophages and hepatocytes in the pathogenesis of obesity-associated NAFLD. In addition, $A_{2A}R$ has a previously unidentified role in repressing sterol regulatory element-binding protein 1c (SREBP1c), which contributes to the anti-steatotic effect of $A_{2A}R$.

MATERIALS AND METHODS

Animal experiments

Wild-type (WT) C57BL/6J were obtained from Jackson Laboratory (Bar Harbor, ME). $A_{2A}R^{-/-}$, $A_{2A}R^{+/-}$, and $A_{2A}R^{+/+}$ mice were generated as described (22). Myeloid cell-specific $A_{2A}R$-disrupted mice were generated using the Cre-LoxP strategy. Briefly, homozygous myeloid cell-specific $A_{2A}R$-disrupted ($LysMCre^{+}$-$A_{2A}R^{F/F}$) mice, heterozygous $A_{2A}R$-disrupted ($LysMCre^{+}$-$A_{2A}R^{F/+}$) mice, and LysM control ($LysMCre^{+}$-$A_{2A}R^{+/+}$) mice were used. All mice were maintained on a 12:12-h light-dark cycle (lights on at 06:00) and subjected to studies involving chow-diet, high-fat diet (HFD, 60% fat calories) and low-fat diet (LFD, 10% fat calories) as detailed in Supplementary Information (SI). All study protocols were reviewed and approved by the Institutional Animal Care and Use Committee of Texas A&M University.

Cell culture and treatment

Bone marrow cells were prepared from $A_{2A}R$-disrupted mice and WT mice, as well as $LysMCre^{+}$-$A_{2A}R^{F/F}$ mice and $LysMCre^{+}$-$A_{2A}R^{+/+}$ mice, and differentiated into macrophages (BMDM) and examined for the proinflammatory activation as described (23). Primary hepatocytes were isolated from free-fed mice (24, 25) and examined for metabolic and inflammatory responses. For macrophage-hepatocyte co-culture study, bone marrow cells were prepared from $A_{2A}R$-disrupted mice and WT mice at 6 days prior to hepatocyte isolation. After differentiation, BMDM were trypsinized and added to WT primary mouse hepatocytes at a ratio of 1:10 based on the published method (12). Some hepatocytes were incubated in the absence of macrophages and served as the control. After incubation for 48 hr, the co-cultures and control

hepatocytes were subjected to the selected assays detailed in SI. Additional experiments involving hepatocytes were also detailed in SI.

Histological, biochemical and molecular assays

Liver sections were subjected to histological and immunohistochemical assays. Plasma parameters were measured using metabolic assay kits and ELISA kits. Also, tissue and/or cell samples were subjected to selected assays including Western blots analysis, real-time PCR, the reporter assays, and chromatin immunoprecipitation (ChIP) assay. Details are provided in SI.

Statistical Methods

Numeric data are presented as means ± SE (standard error). Statistical significance was assessed by unpaired, two-tailed ANOVA or Student's *t* tests. Differences were considered significant at the two-tailed $P < 0.05$.

RESULTS

HFD feeding increases liver $A_{2A}R$ abundance and the proinflammatory status

Tissue distribution results revealed that the liver is one of the organs in which $A_{2A}R$ abundance was at the highest levels (Figure 1A). Next, we examined the pathophysiological relevance of hepatic expression of $A_{2A}R$ in C57BL/6J mice, which display obesity-associated NAFLD upon feeding HFD (9, 10). HFD-fed C57BL/6J mice displayed a significant increase in liver $A_{2A}R$ mRNAs compared to LFD-fed mice (Figure 1B). HFD-fed mice also displayed significant increases in liver protein levels of $A_{2A}R$, as well as CD39 and CD73 (ectoenzymes responsible

for extracellular adenosine production) (Figure 1C). By immunohistochemistry in liver sections, HFD-fed mice revealed increased $A_{2A}R$ expression in liver cells including hepatocytes compared with LFD-fed mice (Supplemental Figure S1). Additionally, HFD-fed C57BL/6J mice displayed significant increases in liver phosphorylation states of Jun N-terminal kinase (JNK) p46 and nuclear factor kappa B (NFκB) p65 as well as mRNA and protein levels of TNFα, interleukin 1 beta (IL-1β), and/or IL-6 compared with LFD-fed mice (Figure 1D,E). These results suggest an association between $A_{2A}R$ amount and diet-induced liver inflammation.

$A_{2A}R$ disruption exacerbates HFD-induced hepatic steatosis and inflammation

The role of $A_{2A}R$ in obesity-associated NAFLD remains largely unknown, and was examined using both male and female $A_{2A}R$-disrupted ($A_{2A}R^{-/-}$ and/or $A_{2A}R^{+/-}$) mice, and their WT ($A_{2A}R^{+/+}$) littermates (Supplemental Figure S2A) upon HFD feeding for 12 weeks. After the feeding period, hepatic $A_{2A}R$ expression was examined and verified for $A_{2A}R$ disruption (Supplemental Figure S2B). Regardless of the gender, $A_{2A}R^{-/-}$ mice displayed much more severe phenotype of insulin resistance and glucose intolerance compared with $A_{2A}R^{+/-}$ mice and/or $A_{2A}R^{+/+}$ mice; although $A_{2A}R$ disruption exacerbated HFD-induced obesity in male, but not female mice (Supplemental Figures S3-S6). Next, we examined the effect of $A_{2A}R$ disruption on NAFLD pathology. Among male mice, HFD-fed $A_{2A}R$-disrupted mice revealed a greater increase in liver weight compared with control mice and this increase was gene-dose-dependent (Figure 2A). Consistently, the severity of HFD-induced hepatic steatosis in $A_{2A}R^{-/-}$ mice or $A_{2A}R^{+/-}$ mice was greater than that in $A_{2A}R^{+/+}$ mice. Also, HFD-induced hepatic steatosis in $A_{2A}R^{-/-}$ mice was much pronounced compared to $A_{2A}R^{+/-}$ mice as demonstrated by H&E or Oil Red O staining in liver sections (Figure 2B). Additionally, both plasma and hepatic levels of

triglycerides in HFD-fed $A_{2A}R^{-/-}$ mice were greater than their respective levels in HFD-fed $A_{2A}R^{+/-}$ mice and/or $A_{2A}R^{+/+}$ mice (Supplemental Figure S7A,B). Among female mice, $A_{2A}R$ disruption caused a slight increase in the severity of HFD-induced hepatic steatosis without significantly altering liver weight (Supplemental Figure S7C).

Because HFD-induced phenotype in male mice was more pronounced, we examined other liver phenotypes, i.e., inflammation and insulin sensitivity, mainly in male mice. Upon HFD feeding, $A_{2A}R$-disrupted and control mice displayed comparable numbers of macrophages/Kupffer cells in the liver (Figure 2B). However, either HFD-fed $A_{2A}R^{-/-}$ mice or HFD-fed $A_{2A}R^{+/-}$ mice revealed a significant increase in liver proinflammatory signaling through JNK p64 and/or NFκB p65 (Figure 2C). The same trends were also observed in TNFα and IL-1β mRNAs (Figure 2D). Since increased lipogenesis is key to the development of hepatic steatosis, we examined the mRNA levels of ACC1 and FAS, which are key enzymes that stimulate liver lipogenesis by converting acetyl-CoA to malonyl-CoA and synthesizing long-chain fatty acids (26, 27). Compared with those in livers of HFD-fed $A_{2A}R^{+/+}$ mice, the mRNA levels of ACC1 and FAS in either HFD-fed $A_{2A}R^{-/-}$ mice or HFD-fed $A_{2A}R^{+/-}$ mice were significantly elevated, and these elevations were $A_{2A}R$ gene-dependent (Figure 2D). Additionally, hepatic mRNA levels of SREBP1c in HFD-fed $A_{2A}R$-disrupted mice were significantly elevated in an $A_{2A}R$ gene-dependent manner (Figure 2D). We also measured hepatic mRNA levels of CPT1a, a master regulator that transfers acyl CoA into mitochondria for oxidation (28, 29). Compared with the control, CPT1a mRNAs in HFD-fed $A_{2A}R^{-/-}$ mice were slightly higher than in HFD-fed $A_{2A}R^{+/+}$ mice or $A_{2A}R^{+/-}$ mice (Figure 2D), suggesting a compensatory response to increased hepatic steatosis. Since SREBP1c stimulates lipogenic gene expression, we analyzed hepatic SREBP1c

expression. Both cytosolic and nuclear SREBP1c levels were significantly increased in HFD-fed $A_{2A}R^{-/-}$ mice compared to the values of HFD-fed $A_{2A}R^{+/+}$ mice (Figure 2E). When insulin signaling was analyzed, insulin-stimulated insulin receptor phosphorylation and Akt phosphorylation (S473) were significantly decreased in HFD-fed $A_{2A}R$-disrupted mice compared to $A_{2A}R^{+/+}$ mice; the decreases were $A_{2A}R$ gene-dose-dependent (Figure 2F). These results suggest that $A_{2A}R$ disruption exacerbates diet-induced hepatic steatosis and inflammation in male mice. Moreover, $A_{2A}R$ disruption enhances liver lipogenic events.

Myeloid cell-specific $A_{2A}R$ disruption exacerbates aspects of NAFLD

Macrophages critically regulate liver inflammation and hepatic steatosis. We sought to address a role for the $A_{2A}R$ in macrophages (myeloid cells) in the pathophysiology of NAFLD. We fed homozygous myeloid cell-specific $A_{2A}R$ disrupted (LysMCre^{+}-$A_{2A}R^{F/F}$) mice, heterozygous myeloid cell-specific $A_{2A}R$ disrupted (LysMCre^{+}-$A_{2A}R^{F/+}$) mice, and their WT (LysMCre^{+}-$A_{2A}R^{+/+}$) littermates (Supplemental Figure S8) an HFD and examined systemic insulin sensitivity and NAFLD aspects. Compared with HFD-fed LysMCre^{+}-$A_{2A}R^{+/+}$ mice, HFD-fed LysMCre^{+}-$A_{2A}R^{F/F}$ mice and HFD-fed LysMCre^{+}-$A_{2A}R^{F/+}$ mice revealed similar increases in the severity of systemic insulin resistance although all mice displayed similar body weight and consumed comparable amount of foods (Supplemental Figures S9 and S10A,B). However, liver weight as well as the severity of HFD-induced hepatic steatosis in LysMCre^{+}-$A_{2A}R^{F/F}$ or LysMCre^{+}-$A_{2A}R^{F/+}$ mice was greater compared to HFD-fed LysMCre^{+}-$A_{2A}R^{+/+}$ mice (Figure 3A,B). Additionally, plasma and hepatic levels of triglycerides in HFD-fed LysMCre^{+}-$A_{2A}R^{F/F}$ mice were significantly greater than their respective levels in HFD-fed LysMCre^{+}-$A_{2A}R^{+/+}$ mice or LysMCre^{+}-$A_{2A}R^{F/+}$ mice (Supplemental Figure S10C,D). The severity of HFD-induced hepatic

steatosis in LysMCre^{+}-$A_{2A}R^{F/F}$ mice was lower compared to that observed in global $A_{2A}R$-deficient ($A_{2A}R^{-/-}$) mice. When liver proinflammatory signaling was examined, the phosphorylation states of JNK p46 and/or NFκB p65 and the mRNA levels of cytokines in HFD-fed LysMCre^{+}-$A_{2A}R^{F/F}$ mice were greater than in HFD-fed HFD-fed LysMCre^{+}-$A_{2A}R^{+/+}$ mice or LysMCre^{+}-$A_{2A}R^{F/+}$ mice (Figure 3C, D). Consistent with increased hepatic steatosis, liver mRNA expression of ACC1 and FAS in HFD-fed LysMCre^{+}-$A_{2A}R^{F/F}$ mice was also greater than their respective levels observed in HFD-fed LysMCre^{+}-$A_{2A}R^{+/+}$ or LysMCre^{+}-$A_{2A}R^{F/+}$ mice (Figure 3D). Taken together, these results suggest that $A_{2A}R$ disruption in macrophages (myeloid cells) is sufficient to exacerbate diet-induced NAFLD.

$A_{2A}R$-disrupted macrophages display increased proinflammatory responses and exacerbate hepatocyte fat deposition and cytokine expression

Since LysMCre^{+}-$A_{2A}R^{F/F}$ mice revealed increased severity of diet-induced NAFLD, we sought to verify a direct role played by the $A_{2A}R$ in macrophages in regulating hepatocyte responses *in vitro*. Initially, we isolated bone marrow cells from $A_{2A}R^{-/-}$ and/or $A_{2A}R^{+/+}$ mice, differentiated the cells into macrophage (BMDM), and analyzed BMDM proinflammatory responses. Under LPS-stimulated conditions, the phosphorylation states of JNK p46 and NFκB p65 as well as the secretion of TNFα and IL-6 were significantly increased in $A_{2A}R^{-/-}$ BMDM compared to the values observed in $A_{2A}R^{+/+}$ BMDM (Figure 4A,B). Similarly, LPS-induced phosphorylation states of JNK p46 and NFκB p65 in BMDM from LysMCre^{+}-$A_{2A}R^{F/F}$ mice were significantly increased compared with those in BMDM from LysMCre^{+}-$A_{2A}R^{+/+}$ mice (Figure 4C).

Next, we co-cultured WT primary mouse hepatocytes with $A_{2A}R^{-/-}$ or $A_{2A}R^{+/+}$ BMDM. Under palmitate-stimulated conditions, hepatocytes co-cultured with $A_{2A}R^{-/-}$ BMDM accumulated more fat and revealed significantly higher levels of triglycerides than hepatocytes co-cultured in the absence of BMDM or in the presence of $A_{2A}R^{+/+}$ BMDM (Figure 5A). When the expression of genes/enzymes related to fat metabolism was analyzed, ACC1, FAS and SREBP1c mRNAs in hepatocytes co-cultured with $A_{2A}R^{-/-}$ BMDM were significantly higher than their respective levels in hepatocytes co-cultured in the absence of BMDM or in the presence of $A_{2A}R^{+/+}$ BMDM (Figure 5B). In contrast, CPT1a mRNAs in hepatocytes co-cultured with $A_{2A}R^{-/-}$ BMDM were significantly lower than those in hepatocytes co-cultured in the absence of BMDM or in the presence of $A_{2A}R^{+/+}$ BMDM. When the expression of cytokines was analyzed, TNFα and IL-1β mRNAs in hepatocytes co-cultured with $A_{2A}R^{-/-}$ BMDM were significant higher than their respective levels in hepatocytes co-cultured in the absence of BMDM or in the presence of $A_{2A}R^{+/+}$ BMDM under basal conditions (Figure 5C, top panel). Strikingly, under LPS-stimulated conditions, TNFα, IL-1β, and IL-6 mRNAs in hepatocytes co-cultured with $A_{2A}R^{+/+}$ or $A_{2A}R^{-/-}$ BMDM were markedly higher than their respective levels in hepatocytes cultured in the absence of BMDM (Figure 5C, bottom panel). Among co-cultures, TNFα, IL-1β, and IL-6 mRNAs in hepatocytes/$A_{2A}R^{-/-}$ BMDM co-cultures were also significantly higher than their respective levels in hepatocytes/$A_{2A}R^{+/+}$ BMDM co-cultures. Additionally, the phosphorylation states of Akt in hepatocytes co-cultured with $A_{2A}R^{-/-}$ BMDM were significantly lower than those in control hepatocytes or control co-cultures (Figure 5D). Taken together, these results suggest that the $A_{2A}R$ in macrophages protects against macrophage proinflammatory activation. The latter has detrimental effects on increasing hepatocyte fat deposition and proinflammatory responses and on impairing hepatocyte insulin sensitivity.

$A_{2A}R$ disruption exacerbates hepatocyte fat deposition and proinflammatory responses

$A_{2A}R$ appeared to play a protective role in NAFLD. Next, we examined the direct effects of $A_{2A}R$ disruption on hepatocyte responses. When fat deposition was analyzed, hepatocytes from $A_{2A}R^{-/-}$ mice accumulated much more fat and revealed significantly higher levels of triglycerides than hepatocytes from $A_{2A}R^{+/-}$ mice or $A_{2A}R^{+/+}$ mice under palmitate-stimulated conditions (Figure 6A). When proinflammatory signaling was analyzed, the phosphorylation states of JNK p46 and NFκB p65 in hepatocytes from $A_{2A}R^{-/-}$ mice were significantly stronger than those in hepatocytes from $A_{2A}R^{+/-}$ mice or $A_{2A}R^{+/+}$ mice under LPS-stimulated conditions (Figure 6B). When insulin sensitivity was analyzed, the states of insulin-stimulated Akt phosphorylation in hepatocytes from $A_{2A}R^{-/-}$ or $A_{2A}R^{+/-}$ mice were significantly lower than those in hepatocytes from $A_{2A}R^{+/+}$ mice (Figure 6C). Consistently, $A_{2A}R$ inhibition increased hepatocyte fat deposition and proinflammatory responses, and decreased hepatocyte insulin signaling (Supplemental Figure S11). Taken together, these results indicate a direct role of $A_{2A}R$ in protecting hepatocytes from palmitate-induced fat deposition and from LPS-induced proinflammatory responses.

$A_{2A}R$ disruption increases the expression and transcription activity of SREBP1c

$A_{2A}R$ disruption exacerbated hepatic steatosis and increased lipogenic events. To gain mechanistic insights for $A_{2A}R$ regulation of lipogenesis, we examined the effect of $A_{2A}R$ disruption on SREBP1c in mice and in isolated primary mouse hepatocytes. Since feeding increases the amount and/or transcription activity of SREBP1c, we examined whether $A_{2A}R$ disruption alters the effect of feeding on SREBP1c. Compared with fasting, feeding caused a

significant increase in the abundance of both cytosolic and nuclear SREBP1c in livers of $A_{2A}R^{+/+}$ mice, but not $A_{2A}R^{-/-}$ mice. Strikingly, the abundance of either cytosolic or nuclear SREBP1c in livers of $A_{2A}R^{-/-}$ mice was greater than that in livers of $A_{2A}R^{+/+}$ mice under fasted conditions, but not fed conditions (Figure 7A). Consistently, the abundance of cytosolic or nuclear SREBP1c was increased in hepatocytes from $A_{2A}R^{-/-}$ mice compared with that in hepatocytes from $A_{2A}R^{+/+}$ mice under conditions mimicking fasting (Figure 7B). We then performed the reporter assay and observed that SREBP1c transcription activity in hepatocytes from $A_{2A}R^{-/-}$ mice was significantly higher than that in hepatocytes from $A_{2A}R^{+/+}$ mice under basal conditions (in the absence of insulin) (Figure 7C). Similar changes were also observed in hepatocytes under insulin-stimulated conditions. However, insulin increased SREBP1c transcription activity in hepatocytes from $A_{2A}R^{+/+}$ but not $A_{2A}R^{-/-}$ mice. Next, we performed the ChIP assay. The binding of SREBP1c to SRE/E (a binding element in FAS promoter region) was significantly increased in nuclear extracts of hepatocytes from $A_{2A}R^{-/-}$ mice compared with that observed in hepatocytes from $A_{2A}R^{+/+}$ mice (Figure 7C). Also, the mRNAs of key target genes of SREBP1c, e.g., glucokinase and FAS, were greater in hepatocytes from $A_{2A}R^{-/-}$ mice compared to those of hepatocytes from $A_{2A}R^{+/+}$ mice (Figure 7D). These results suggest that $A_{2A}R$ is capable of repressing SREBP1c expression under fasted conditions and suppressing SREBP1c transcription activity.

We also examined the phosphorylation status of AMP-activated protein kinase (AMPK), a regulator that exerts a powerful anti-steatotic effect. Compared with those in HFD-fed $A_{2A}R^{+/+}$ mice or $A_{2A}R^{+/-}$ mice, hepatic phosphorylation states of AMPK in HFD-fed $A_{2A}R^{-/-}$ mice were significantly decreased (Figure 7E). Since cellular ADP: ATP ratio critically influences AMPK phosphorylation, we performed cellular assays and observed that the ADP: ATP ratios were

significantly lower in hepatocytes from $A_{2A}R^{-/-}$ mice than those of hepatocytes from $A_{2A}R^{+/+}$ mice or $A_{2A}R^{+/-}$ mice (Figure 7F). These results were consistent with changes in the status of hepatic steatosis.

DISCUSSION

We established an association between $A_{2A}R$ and obesity-associated NAFLD using HFD-fed WT mice, in which increased liver proinflammatory responses were accompanied by increased liver abundance of $A_{2A}R$. Considering that $A_{2A}R$ activation exerts powerful anti-inflammatory effects (19, 20, 30, 31) whereas $A_{2A}R$ deficiency exacerbates proinflammatory responses (32), we speculated that the increase in liver $A_{2A}R$ abundance in HFD-fed WT mice was a defensive response. As substantial evidence, global $A_{2A}R$ deficient mice displayed a significant increase in the severity of HFD-induced liver inflammation and other NAFLD aspects. Of importance, this evidence from $A_{2A}R$ deficient mice establishes a cause-and-effect relationship between $A_{2A}R$ disruption and NAFLD. In global $A_{2A}R$-deficient mice, increased NAFLD aspects may be attributable to the lack of $A_{2A}R$ in macrophages, hepatocytes, or both. Considering the importance of macrophages in regulating inflammation, we speculated that the $A_{2A}R$ in macrophages was needed for protecting mice from obesity-associated NAFLD and we found this was the case. Therefore, our three lines of *in vivo* evidence makes it conceivable that $A_{2A}R$ acts through, at least partially, suppressing inflammation to protect against obesity-associated NAFLD.

$A_{2A}R$ activation was previously shown to ameliorate methionine- and choline-deficient diet (MCD)-induced NASH in rats (19). A follow-up study confirmed the beneficial effect of $A_{2A}R$ activation in MCD-fed mice (20), which was associated with decreased proinflammatory responses in both hepatocytes and lymphocytes. These results suggest anti-inflammation as an essential mechanism by which $A_{2A}R$ activation improves NASH. However, the studies by Carini et al. did not address how macrophages respond to $A_{2A}R$ activation in the context of protecting against NASH. Indeed, the observed decreases in cytokine production by hepatic mononuclear cells of MCD-fed mice upon $A_{2A}R$ activation could be secondary to the anti-inflammatory effects of $A_{2A}R$ activation on hepatocytes and/or macrophages. Considering that macrophages have been implicated to critically determine the development and progression of obesity-associated NAFLD (11, 12), it is necessary to address how the $A_{2A}R$ in macrophages alters NAFLD aspects. In the present study, we confirmed that $A_{2A}R$ disruption exacerbates macrophage proinflammatory activation. Moreover, we revealed, for the first time, that myeloid cell-specific $A_{2A}R$ deficiency exacerbated HFD-induced hepatic steatosis and inflammation. Because $A_{2A}R$ was disrupted only in myeloid cells, increased hepatic steatosis and inflammation in HFD-fed $LysMCre^{+}$-$A_{2A}R^{F/F}$ mice appeared to be secondary to the consequences of $A_{2A}R$ disruption in myeloid cells. As supporting evidence, hepatocytes co-cultured with $A_{2A}R$-disrupted macrophages revealed significant increases in the expression of proinflammatory cytokines and in palmitate-induced fat deposition and in the expression of ACC1, FAS, and SREBP1c compared with hepatocytes co-cultured with control macrophages. Because the initial differences among co-cultures existed solely in macrophages (e.g., the presence or absence of $A_{2A}R$), the outcomes of hepatocyte lipogenic events were attributable to the effects secondary to $A_{2A}R$ disruption-associated increase in macrophage proinflammatory activation. The latter has

been previously shown to generate macrophage-derived factors, i.e., proinflammatory cytokines, to promote hepatocyte lipogenic events (14), enhance hepatocyte proinflammatory responses, and decrease hepatocyte insulin signaling (33). Therefore, the results from myeloid cell-specific $A_{2A}R$ deficient mice and macrophage-hepatocyte co-cultures demonstrated that $A_{2A}R$ has a role in coordinating macrophage actions on hepatocytes to protect against NAFLD aspects.

$A_{2A}R$ also critically regulates hepatocyte metabolic and inflammatory responses. In support of this, $A_{2A}R$ disruption brought about deleterious effects on palmitate-induced fat deposition and on LPS-induced proinflammatory responses in primary mouse hepatocytes. In addition, treatment of WT mouse hepatocytes with an $A_{2A}R$ antagonist generated effects mimicking $A_{2A}R$ disruption. These two lines of evidence not only recapitulated the findings in HFD-fed $A_{2A}R$-disrupted mice, but also served as complementary evidence to support the anti-inflammatory and anti-steatotic effects of $A_{2A}R$ activation (19, 20). However, it remains to be explored, within hepatocytes, whether and how the anti-inflammatory effect of $A_{2A}R$ interplays with the anti-lipogenic effect of $A_{2A}R$. Given the co-existence of these effects of $A_{2A}R$, it is possible that $A_{2A}R$ acts through suppressing hepatocyte inflammatory signaling to inhibit lipogenic events. Alternatively, $A_{2A}R$ may act through two parallel pathways to suppress hepatocyte proinflammatory responses and to inhibit hepatocyte fat deposition.

It is a significant finding that $A_{2A}R$ disruption elevated hepatic SREBP1c abundancy. Additionally, increased liver abundancy of SREBP1c in HFD-fed $A_{2A}R$-deficient mice was accompanied with increases in hepatic expression of lipogenic enzymes and in the severity of hepatic steatosis. These results are consistent with an established paradigm concerning the

critical contribution of lipogenesis, at increased levels, to the development of hepatic steatosis (34-36). Physiologically, hepatic SREBP1c is stimulated by feeding and repressed by fasting (36), which accounts for increased hepatic fat content under fed states and decreased hepatic fat content under fasted states, respectively. Strikingly and interestingly, in the present study, $A_{2A}R$ deficiency increased liver SREBP1c abundance under fasted conditions, where SREBP1c expression and activity should be suppressed physiologically. Consistently, $A_{2A}R$ disruption increased the abundance of SREBP1c in hepatocytes upon nutrient deprivation. These findings support a repressive effect $A_{2A}R$ on SREBP1c. Additional to altering SREBP1c abundance, $A_{2A}R$ disruption also decreased hepatic AMPK phosphorylation states, likely through a mechanism involving decreases in hepatocyte ADP: ATP ratio because AMPK is activated by increased ratios of AMP: ATP and ADP: ATP. Considering the role of AMPK in phosphorylating and inactivating SREBP1c (37), $A_{2A}R$ deficiency-associated decreases in AMPK phosphorylation appeared to also contribute to the effects of $A_{2A}R$ deficiency on increasing hepatic lipogenesis and on exacerbating hepatic steatosis. Indeed, at the cellular level, $A_{2A}R$ disruption increased SREBP1c transcription activity and enhanced the binding of SREBP1c to the promoter region of FAS. Collectively, our findings suggest that $A_{2A}R$ signaling pathways are involved in repression of SREBP1c, which in turn contributes to the effects of $A_{2A}R$ on suppressing lipogenic events, and on protecting against the development of hepatic steatosis.

In summary, we validated a protective role for $A_{2A}R$ in obesity-associated NAFLD. Mechanistically, this role of $A_{2A}R$ is attributable to the direct effects of $A_{2A}R$ on altering inflammatory and metabolic responses of macrophages and hepatocytes. Specifically, $A_{2A}R$

suppresses macrophage and hepatocyte proinflammatory responses. $A_{2A}R$ suppression of macrophage activation also generates secondary effects on inhibiting the inflammatory responses and lipogenic events of hepatocytes. Lastly, $A_{2A}R$ can directly suppress hepatocyte fat deposition, which is attributable to the effects of $A_{2A}R$ on repressing SREBP1c expression under fasted states and on suppressing SREBP1c transcription activity. Therefore, targeting $A_{2A}R$ to suppress inflammation and lipogenesis is a viable therapeutic strategy for the treatment of NAFLD and inflammation-associated human liver diseases.

FUNDING

This work was supported in whole or in part by grants from the American Diabetes Association (1-17-IBS-145 to C.W.) and the National Institutes of Health (DK095862 to C.W. and HL095556 to Y.H). This work was also supported in part by the Dr. Nicholas C. Hightower Centennial Chair of Gastroenterology from Scott & White, a VA Research Career Scientist Award to G.A. and the NIH grants DK062975 and DK054811 to Drs. G.A, F.M. and S.G. Also, C.W. is supported by the Hatch Program of the National Institutes of Food and Agriculture (NIFA). Y.C. is supported by China Scholarship Council.

AUTHOR CONTRIBUTION

Y.C. carried out most of experiments involving mice. H.L. and M.L. carried out most of experiments involving cells. Y.P., J. Zheng, J. Zhou, X.L., W.H. L.M., and Q.Y. collected tissue and cell samples and performed molecular and biochemical assays. Y.H. G.A., and C.W. came up the concept of the study. S. Guo, X.X., Q.L., T.Z., F.M., H.F., S. Glaser, L.C., Y.H., and G.A. contributed to scientific discussion. C.W. supervised all experiments and wrote the manuscript.

CONFLICT OF INTEREST

This material, in part, is the result of work supported with resources and the use of facilities at the Central Texas Veterans Health Care System, Temple, Texas. The content is the responsibility of the author(s) alone and does not necessarily reflect the views or policies of the Department of Veterans Affairs or the United States Government.

REFERENCES

1. Browning JD, Szczepaniak LS, Dobbins R, Nuremberg P, Horton JD, Cohen JC, Grundy SM, et al. Prevalence of hepatic steatosis in an urban population in the United States: Impact of ethnicity. Hepatology 2004;40:1387-1395.

2. Sanyal AJ. Mechanisms of Disease: pathogenesis of nonalcoholic fatty liver disease. Nat Clin Pract Gastroenterol Hepatol 2005;2:46-53.

3. Cohen JC, Horton JD, Hobbs HH. Human fatty liver disease: old questions and new insights. Science 2011;332:1519-1523.

4. Tilg H, Kaser A. Treatment strategies in nonalcoholic fatty liver disease. Nat Clin Pract Gastroenterol Hepatol 2005;2:148-155.

5. Tilg H, Moschen AR. Evolution of inflammation in nonalcoholic fatty liver disease: The multiple parallel hits hypothesis. Hepatology 2010;52:1836-1846.

6. Targher G, Bertolini L, Poli F, Rodella S, Scala L, Tessari R, Zenari L, et al. Nonalcoholic fatty liver disease and risk of future cardiovascular events among type 2 diabetic patients. Diabetes 2005;54:3541-3546.

7. Kotronen A, Yki-Jarvinen H. Fatty Liver: A novel component of the metabolic syndrome. Arterioscler Thromb Vasc Biol 2008;28:27-38.

8. Farrell GC, Larter CZ. Nonalcoholic fatty liver disease: From steatosis to cirrhosis. Hepatology 2006;43:S99-S112.

9. Woo S-L, Xu H, Li H, Zhao Y, Hu X, Zhao J, Guo X, et al. Metformin ameliorates hepatic steatosis and inflammation without altering adipose phenotype in diet-induced obesity. PLoS ONE 2014;9:e91111.

10. Guo T, Woo S-L, Guo X, Li H, Zheng J, Botchlett R, Liu M, et al. Berberine ameliorates hepatic steatosis and suppresses liver and adipose tissue inflammation in mice with diet-induced obesity. Sci Rep 2016;6:22612.

11. Kang K, Reilly SM, Karabacak V, Gangl MR, Fitzgerald K, Hatano B, Lee C-H. Adipocyte-derived Th2 cytokines and myeloid PPARd regulate macrophage polarization and insulin sensitivity. Cell Metab 2008;7:485-495.

12. Odegaard JI, Ricardo-Gonzalez RR, Red Eagle A, Vats D, Morel CR, Goforth MH, Subramanian V, et al. Alternative M2 activation of Kupffer cells by PPARd ameliorates obesity-induced insulin resistance. Cell Metab 2008;7:496-507.

13. Menghini R, Menini S, Amoruso R, Fiorentino L, Casagrande V, Marzano V, Tornei F, et al. Tissue inhibitor of metalloproteinase 3 deficiency causes hepatic steatosis and adipose tissue inflammation in mice. Gastroenterology 2009;136:663-672.e664.

14. Liu C, Rajapakse AG, Riedo E, Fellay B, Bernhard M-C, Montani J-P, Yang Z, et al. Targeting arginase-II protects mice from high-fat-diet-induced hepatic steatosis through suppression of macrophage inflammation. Scientific Reports 2016;6:20405.

15. Haskó G, Linden J, Cronstein B, Pacher P. Adenosine receptors: therapeutic aspects for inflammatory and immune diseases. Nat Rev Drug Discov 2008;7:759-770.

16. Gessi S, Varani K, Merighi S, Ongini E, Borea PA. A_{2A} adenosine receptors in human peripheral blood cells. Br J Pharmacol 2000;129:2-11.

17. Ohta A, Sitkovsky M. Role of G-protein-coupled adenosine receptors in downregulation of inflammation and protection from tissue damage. Nature 2001;414:916-920.

18. Peng Z, Borea PA, Wilder T, Yee H, Chiriboga L, Blackburn MR, Azzena G, et al. Adenosine signaling contributes to ethanol-induced fatty liver in mice. J Clin Invest 2009;119:582-594.

19. Imarisio C, Alchera E, Sutti S, Valente G, Boccafoschi F, Albano E, Carini R. Adenosine A2a receptor stimulation prevents hepatocyte lipotoxicity and nonalcoholic steatohepatitis (NASH) in rats. Clin Sci 2012;123:323-332.

20. Alchera E, Rolla S, Imarisio C, Bardina V, Valente G, Novelli F, Carini R. Adenosine A2a receptor stimulation blocks development of nonalcoholic steatohepatitis in mice by multilevel inhibition of signals that cause immunolipotoxicity. Translational Research 2017;182:75-87.

21. Chiang DJ, Roychowdhury S, Bush K, McMullen MR, Pisano S, Niese K, Olman MA, et al. Adenosine 2A receptor antagonist prevented and reversed liver fibrosis in a mouse model of ethanol-exacerbated liver fibrosis. PLoS ONE 2013;8:e69114.

22. Chen J-F, Huang Z, Ma J, Zhu J, Moratalla R, Standaert D, Moskowitz MA, et al. A_{2A} adenosine receptor deficiency attenuates brain injury induced by transient focal ischemia in mice. J Neurosci 1999;19:9192-9200.

23. Xu H, Li H, Woo S-L, Kim S-M, Shende VR, Neuendorff N, Guo X, et al. Myeloid cell-specific disruption of Period1 and Period2 exacerbates diet-induced inflammation and insulin resistance. J Biol Chem 2014;289:16374-16388.

24. Wu C, Kang JE, Peng L, Li H, Khan SA, Hillard CJ, Okar DA, et al. Enhancing hepatic glycolysis reduces obesity: Differential effects on lipogenesis depend on site of glycolytic modulation. Cell Metab 2005;2:131-140.

25. Bu SY, Mashek MT, Mashek DG. Suppression of long chain acyl-CoA synthetase 3 decreases hepatic de novo fatty acid synthesis through decreased transcriptional activity. J Biol Chem 2009;284:30474-30483.

26. Browning JD, Horton JD. Molecular mediators of hepatic steatosis and liver injury. J Clin Invest 2004;114:147-152.

27. Hillgartner FB, Salati LM, Goodridge AG. Physiological and molecular mechanisms involved in nutritional regulation of fatty acid synthesis. Physiol Rev 1995;75:47-76.

28. Chien D, Dean D, Saha AK, Flatt JP, Ruderman NB. Malonyl-CoA content and fatty acid oxidation in rat muscle and liver in vivo. Am J Physiol Endocrinol Metab 2000;279:E259-265.

29. Rasmussen BB, Holmback UC, Volpi E, Morio-Liondore B, Paddon-Jones D, Wolfe RR. Malonyl coenzyme A and the regulation of functional carnitine palmitoyltransferase-1 activity and fat oxidation in human skeletal muscle. J Clin Invest 2002;110:1687-1693.

30. Odashima M, Bamias G, Rivera-Nieves J, Linden J, Nast CC, Moskaluk CA, Marini M, et al. Activation of A_{2A} adenosine receptor attenuates intestinal inflammation in animal models of inflammatory bowel disease. Gastroenterology 2005;129:26-33.

31. Awad AS, Huang L, Ye H, Duong ETA, Bolton WK, Linden J, Okusa MD. Adenosine A_{2A} receptor activation attenuates inflammation and injury in diabetic nephropathy. Am J Physiol Renal Physiol 2006;290:F828-837.

32. Lukashev D, Ohta A, Apasov S, Chen J-F, Sitkovsky M. Cutting edge: Physiologic attenuation of proinflammatory transcription by the G_s protein-coupled A2A adenosine receptor in vivo. J Immunol 2004;173:21-24.

33. Pardo V, González-Rodríguez Á, Guijas C, Balsinde J, Valverde ÁM. Opposite cross-talk by oleate and palmitate on insulin signaling in hepatocytes through macrophage activation. Journal of Biological Chemistry 2015;290:11663-11677.

34. Shimomura I, Bashmakov Y, Horton JD. Increased levels of nuclear SREBP-1c associated with fatty livers in two mouse models of diabetes mellitus. J Biol Chem 1999;274:30028-30032.

35. Guo X, Li H, Xu H, Halim V, Zhang W, Wang H, Ong KT, et al. Palmitoleate induces hepatic steatosis but suppresses liver inflammatory response in mice. PLoS ONE 2012;7:e39286.

36. Zhao X, Feng D, Wang Q, Abdulla A, Xie X-J, Zhou J, Sun Y, et al. Regulation of lipogenesis by cyclin-dependent kinase 8–mediated control of SREBP-1. The Journal of Clinical Investigation 2012;122:2417-2427.

37. Li Y, Xu S, Mihaylova MM, Zheng B, Hou X, Jiang B, Park O, et al. AMPK phosphorylates and inhibits SREBP activity to attenuate hepatic steatosis and atherosclerosis in diet-induced insulin-resistant mice. Cell Metabolism 2011;13:376-388.

FIGURE LEGENDS

Figure 1. HFD feeding increases hepatic A_{2A}R abundance and enhances liver proinflammatory responses

Wild type C57BL/6J mice were fed as described in Methods. (**A**) Tissue distribution of $A_{2A}R$. SI, small intestine; WAT, white adipose tissue. (**B**) Liver $A_{2A}R$ mRNA levels. AU, arbitrary unit. (**C**) Liver amount of $A_{2A}R$, CD39 (ecto-nucleoside triphosphate diphosphohydrolase 1), and CD73 (ecto-5'-nucleotidase). (**D**) Liver proinflammatory signaling. (**E**) Liver cytokine mRNA (left panel) and protein (right two panels) levels. For A, C, and D, liver lysates were used for Western blot analysis. Blots were quantified using densitometry (bar graphs in C and D). For B and E, liver mRNAs were quantified using real-time RT-PCR. For E, liver protein levels of cytokines were quantified using ELISA kits. For all bar graphs, data are means ± SE. n = 6 - 8. Statistical difference between HFD and LFD: *, $P < 0.05$ and **, $P < 0.01$ in B and E (right two panels) or in bar graphs of C, D, and E (left two panels) for the same protein or gene.

Figure 2. $A_{2A}R$ disruption exacerbates HFD-induced hepatic steatosis and inflammation

Male $A_{2A}R^{-/-}$ mice, $A_{2A}R^{+/-}$ mice, and $A_{2A}R^{+/+}$ mice, at 5 - 6 weeks of age, were fed an HFD for 12 weeks. Age- and gender-matched $A_{2A}R^{+/+}$ mice were fed an LFD for 12 weeks and served as normal control. (**A**) Liver weight. (**B**) Representative images of H&E, Oil-Red-O, and/or F4/80 staining for liver sections. (**C**) Liver proinflammatory signaling. (**D**) Liver mRNA levels. (**E**) Liver SREBP1c abundance. pSREBP1c, precursor SREBP1c; nSREBP1c, nuclear SREBP1c. (**F**) Liver insulin signaling. Prior to tissue harvest, HFD-fed mice were injected with or without insulin (1 U/kg) into the portal vein for 5 min. IR, insulin receptor. For C, E, and F, liver lysates (C and F), as well as liver cytosolic and nuclear fractions (E) were subjected to Western blot analysis. Bar graphs, quantification of blots. For A - F, numeric data are means ± SE. n = 10 - 12 (A) or n = 8 - 10 (C - F). Statistical difference between $A_{2A}R^{-/-}$-HFD and $A_{2A}R^{+/+}$-HFD: *, $P < 0.05$ and **, $P < 0.01$ in bar graphs of A, C, and E, in D within the same gene, or in bar graphs of

F under insulin-stimulated condition; statistical difference between $A_{2A}R^{-/-}$-HFD and $A_{2A}R^{+/-}$-HFD: †, $P < 0.05$ and ††, $P < 0.01$ in bar graphs of A, C, and E, in D within the same gene, or in bar graphs of F under insulin-stimulated condition; statistical difference between $A_{2A}R^{+/-}$-HFD and $A_{2A}R^{+/+}$-HFD: ‡, $P < 0.05$ and ‡‡, $P < 0.01$ in bar graphs of A and C, in D within the same gene, or in bar graphs of F under insulin-stimulated condition.

Figure 3. Myeloid cell-specific $A_{2A}R$ disruption exacerbates HFD-induced hepatic steatosis and proinflammatory responses

Male LysMCre^{+}-$A_{2A}R^{F/F}$ mice, LysMCre^{+}-$A_{2A}R^{F/+}$ mice, and LysMCre^{+}-$A_{2A}R^{+/+}$ mice, at 5 - 6 weeks of age, were fed an HFD for 12 weeks. (**A**) Liver weight. (**B**) Representative images of H&E, Oil-Red-O, and/or F4/80 staining for liver sections. (**C**) Liver lysates were examined for the proinflammatory signaling using Western blot analysis. Bar graphs, quantification of blots. AU, arbitrary unit. TLR4, Toll-like receptor 4. (**D**) Liver mRNA levels were quantified using real-time RT-PCR. For A, C, and D, numeric data are means ± SE. n = 8 - 10. Statistical difference between LysMCre^{+}-$A_{2A}R^{F/F}$ and LysMCre^{+}-$A_{2A}R^{+/+}$: *, $P < 0.05$ and **, $P < 0.01$ in A or in bar graphs of C and D within the same protein or gene; statistical difference between LysMCre^{+}-$A_{2A}R^{F/F}$ and LysMCre^{+}-$A_{2A}R^{F/+}$: †, $P < 0.05$ and ††, $P < 0.01$ in bar graphs of C and D within the same protein or gene; statistical difference between LysMCre^{+}-$A_{2A}R^{F/+}$ and LysMCre^{+}-$A_{2A}R^{+/+}$: ‡, $P < 0.05$ and ‡‡, $P < 0.01$ in A or in bar graphs of C and D within the same protein or gene.

Figure 4. $A_{2A}R$ disruption aggravates macrophage proinflammatory activation.

Bone marrow-derived macrophages (BMDM) were prepared as described in Methods. (**A**, **B**) Proinflammatory signaling (A) and cytokine production (B) of BMDM from $A_{2A}R^{-/-}$ mice and $A_{2A}R^{+/+}$ mice. For A, BMDM were treated with or without lipopolysaccharide (LPS, 100 ng/ml) for 30 min prior to harvest. Cell lysates were subjected to Western blot analysis. Bar graphs, quantification of blots. For B, cytokine concentrations in BMDM conditioned-media. (**C**) Proinflammatory signaling of BMDM from LysMCre^{+}-$A_{2A}R^{F/F}$ mice and LysMCre^{+}-$A_{2A}R^{+/+}$ mice. Cells were treated and analyzed as described in A. Bar graphs, quantification of blots. For A - C, numeric data are means ± SE. n = 4 - 6. Statistical difference between $A_{2A}R^{-/-}$ and $A_{2A}R^{+/+}$: *, $P < 0.05$ and **, $P < 0.01$ in bar graphs of A (under LPS-stimulated condition) or in B; statistical difference between LysMCre^{+}-$A_{2A}R^{F/F}$ and LysMCre^{+}-$A_{2A}R^{+/+}$: †, $P < 0.05$ and ††, $P < 0.01$ in bar graphs of C (under LPS-stimulated condition).

Figure 5. $A_{2A}R$ disruption exacerbates the effects of macrophages on increasing hepatocyte fat deposition, cytokine expression, and insulin resistance

Macrophage-hepatocyte co-cultures were performed as described in Methods. A set of primary hepatocytes were incubated without macrophages and followed by the same treatments as co-cultures. (**A**) Hepatocyte fat deposition. The cells were treated with palmitate (Pal, 250 μM, conjugated in bovine serum albumin (BSA)) or BSA for the last 24 hr of the 48 hr incubation period, and stained with Oil Red O for 1 hr. Bar graphs, quantification of fat content and triglyceride levels. (**B**, **C**) The mRNA levels of genes related to fat metabolism (B) and proinflammatory cytokines (C) were examined using real-time RT-PCR. Prior to harvest, cells were treated without or with LPS (20 ng/ml) for 6 hr. (**D**) Insulin signaling. Prior to harvest, cells were treated with insulin (100 nM) or PBS for 30 min. Cell lysates were subjected to Western

blot analysis. Bar graph, quantification of blots. For A - D, numeric data are means ± SE, n = 4 - 6. Statistical difference between co-cultures with $A_{2A}R^{-/-}$ BMDM and co-cultures with $A_{2A}R^{+/+}$ BMDM: *, $P < 0.05$ and **, $P < 0.01$ in A, in B and C within the same gene, or in bar graph of D under insulin-stimulated condition; statistical difference between co-cultures with $A_{2A}R^{-/-}$ BMDM and hepatocytes cultured without BMDM (None): †, $P < 0.05$ and ††, $P < 0.01$ in A, in B and C within the same gene, or in bar graph of D under insulin-stimulated condition; statistical difference between co-cultures with $A_{2A}R^{+/+}$ BMDM and hepatocytes/None: ‡, $P < 0.05$ in bar graph of D under insulin-stimulated condition.

Figure 6. $A_{2A}R$ disruption exacerbates hepatocyte fat deposition and proinflammatory responses and impairs hepatocyte insulin sensitivity

Primary hepatocytes were isolated from chow-diet-fed male $A_{2A}R^{-/-}$ mice, $A_{2A}R^{+/-}$ mice, and $A_{2A}R^{+/+}$ mice, at 10 - 12 weeks of age. (**A**) Hepatocyte fat deposition. After attachment, hepatocytes were treated with palmitate (Pal, 250 μM) or BSA for 24 hr, and stained with Oil Red O for 1 hr. Bar graphs, quantification of fat content and triglyceride levels. (**B**, **C**) Hepatocyte proinflammatory (B) and insulin (C) signaling. Prior to harvest, cells were treated with LPS (100 ng/ml), insulin (100 nM), or PBS for 30 min. Cell lysates were subjected to Western blot analysis. For A - C, numeric data are means ± SE, n = 4 - 6. Statistical difference between $A_{2A}R^{-/-}$ vs. $A_{2A}R^{+/+}$: *, $P < 0.05$ and **, $P < 0.01$ in A, in B under LPS-stimulated condition, or in C under insulin-stimulated condition; statistical difference between $A_{2A}R^{-/-}$ and $A_{2A}R^{+/-}$: †, $P < 0.05$ in A or in B under LPS-stimulated condition; statistical difference between $A_{2A}R^{+/-}$ and $A_{2A}R^{+/+}$: ‡‡, $P < 0.01$ in C under insulin-stimulated condition.

Figure 7. $A_{2A}R$ deficiency elevates hepatic abundance of SREBP1c under fasting/nutrient deprivation and enhances SREBP1c transcription activity

(**A**) Liver SREBP1c abundance. Male $A_{2A}R^{-/-}$ mice and $A_{2A}R^{+/+}$ mice, at 10 - 12 weeks of age, were free-fed or fasted for 18 hr. (**B**) Hepatocyte SREBP1c abundance. Primary hepatocytes were incubated in M199 in the absence of fetal bovine serum for 24 hr. For A and B, liver (A) or hepatocyte (B) cytosolic and nuclear proteins were subjected to Western blot analysis. (**C**) Hepatocyte SREBP1c transcription activity. Left panel, primary hepatocytes were incubated in M199 in the absence of fetal bovine serum and transfected with a reporter construct in which luciferase expression is under the control of SRE sequences on fatty acid synthase (pFAS-SRE-luc) or a control (pGL3-luc) for 24 hr; right panel, primary hepatocytes were treated as described in B. Hepatocyte chromatins were immunoprecipitated with antibodies against SREBP1c. The resultant DNA were analyzed for SRE/E sequences of FAS promoter. (**D**) Hepatocyte mRNAs. Cells were treated as described in B. (**E**) Liver AMPK phosphorylation states. Male $A_{2A}R^{-/-}$ mice, $A_{2A}R^{+/-}$ mice, and $A_{2A}R^{+/+}$ mice were fed as described in Figure 2. (**F**) Hepatocyte ADP/ATP ratio. Cells were treated as described in B. For B - D and F, primary hepatocytes were isolated from chow-diet-fed male $A_{2A}R^{-/-}$ mice and $A_{2A}R^{+/+}$ mice, at 10 - 12 weeks of age. For A, B, and E, blots were quantified using densitometry. For all bar graphs, data are means ± SE, n = 4 - 6 (in A - C) or n = 6 - 8 (in D - F). Statistical difference between $A_{2A}R^{-/-}$ and $A_{2A}R^{+/+}$: *, $P < 0.05$ and **, $P < 0.01$ in A and B for the same fraction, in C for the same construct under the same condition, in D for the same gene, or in E and F; statistical difference between $A_{2A}R^{-/-}$ and $A_{2A}R^{+/-}$: †, $P < 0.05$ in E and F; statistical difference between insulin-treated $A_{2A}R^{+/+}$ cells and

control-treated $A_{2A}R^{+/+}$ cells (transfected with pFAS-SRE-luc): ‡, $P < 0.05$ in C; statistical difference between $A_{2A}R^{+/-}$ and $A_{2A}R^{+/+}$: ‡‡, $P < 0.01$ in F.

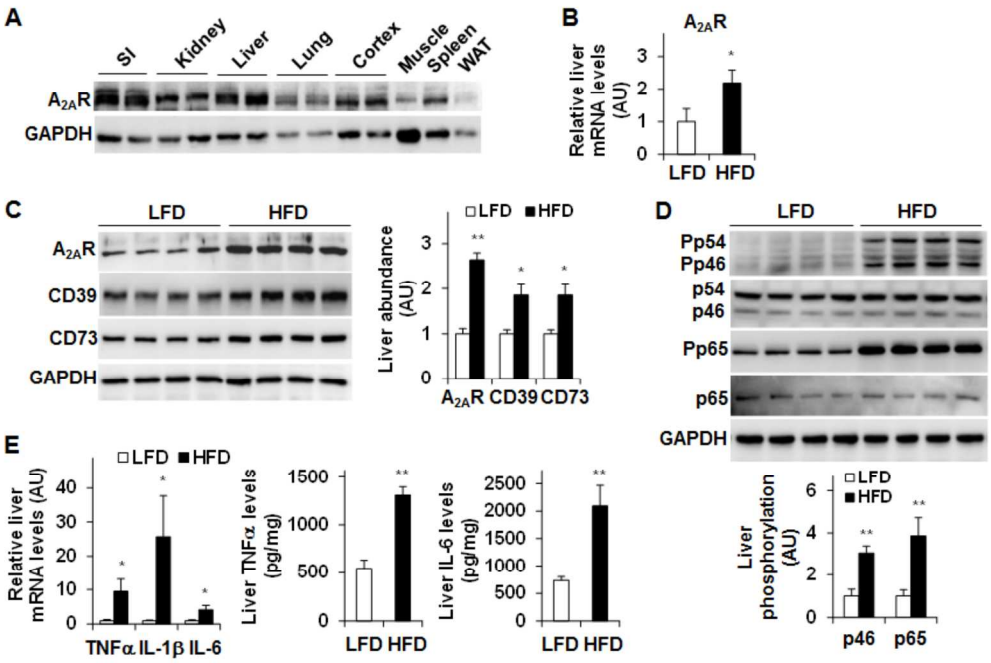

Fig. 1

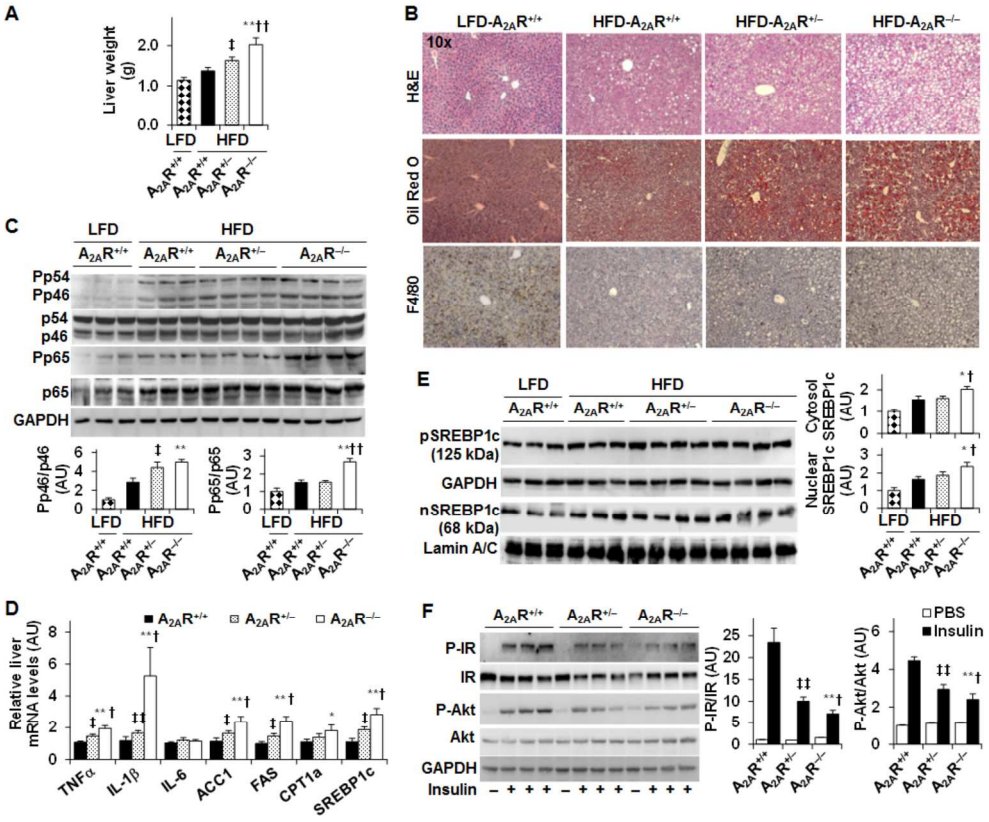

Fig. 2

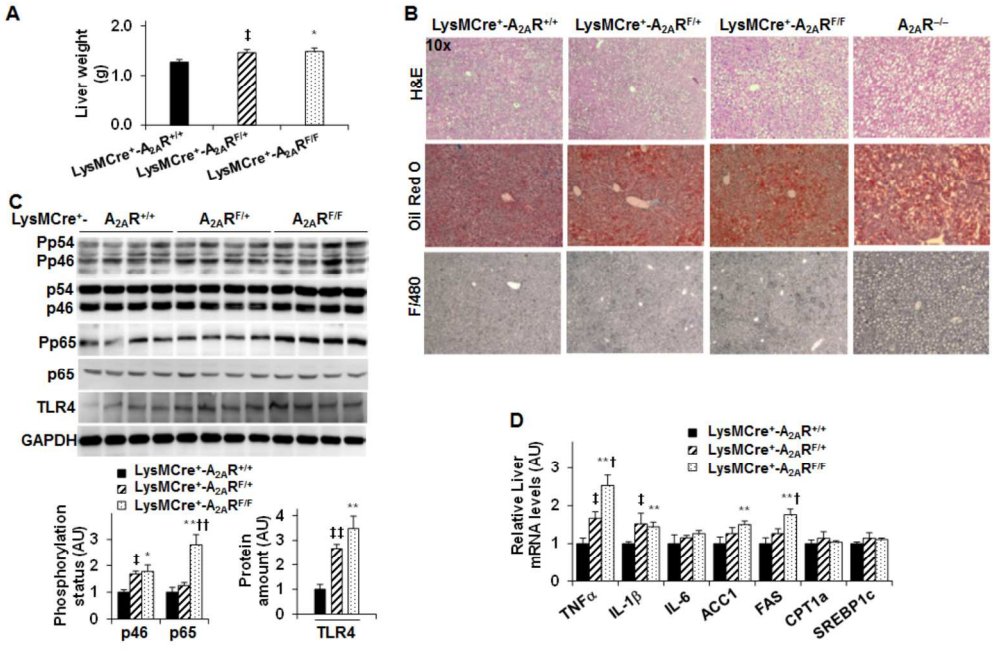

Fig. 3

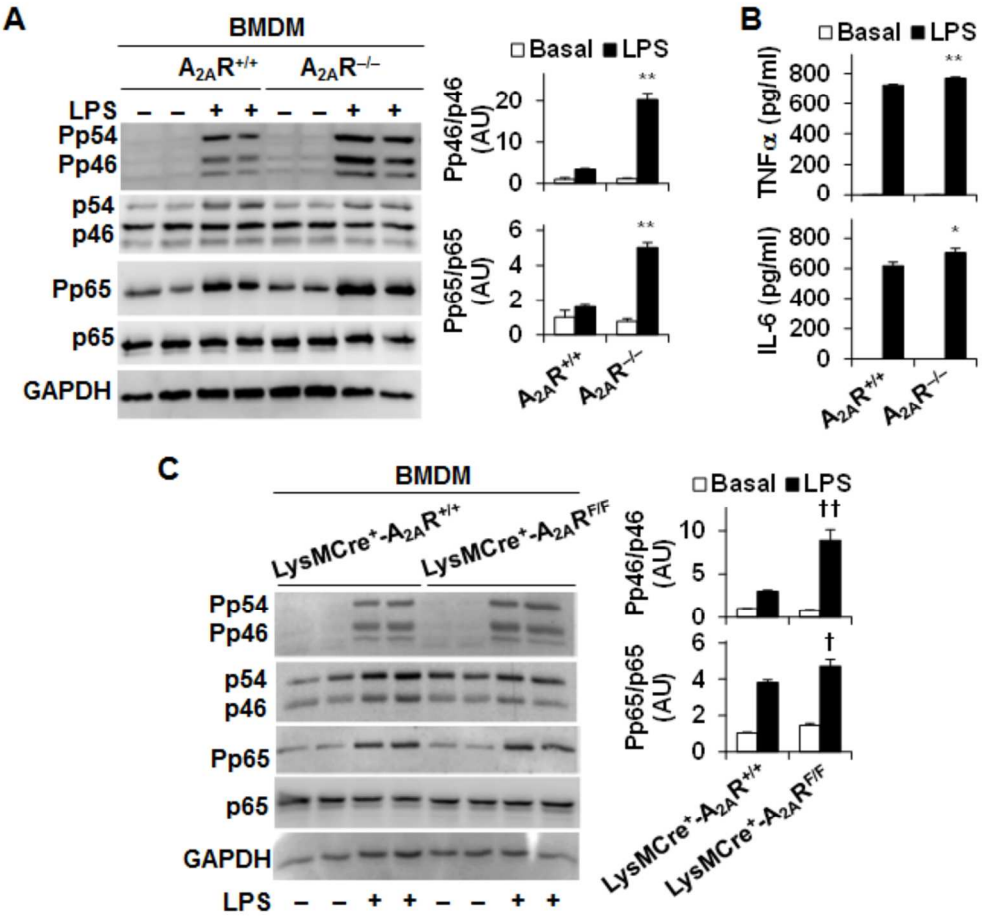

Fig. 4

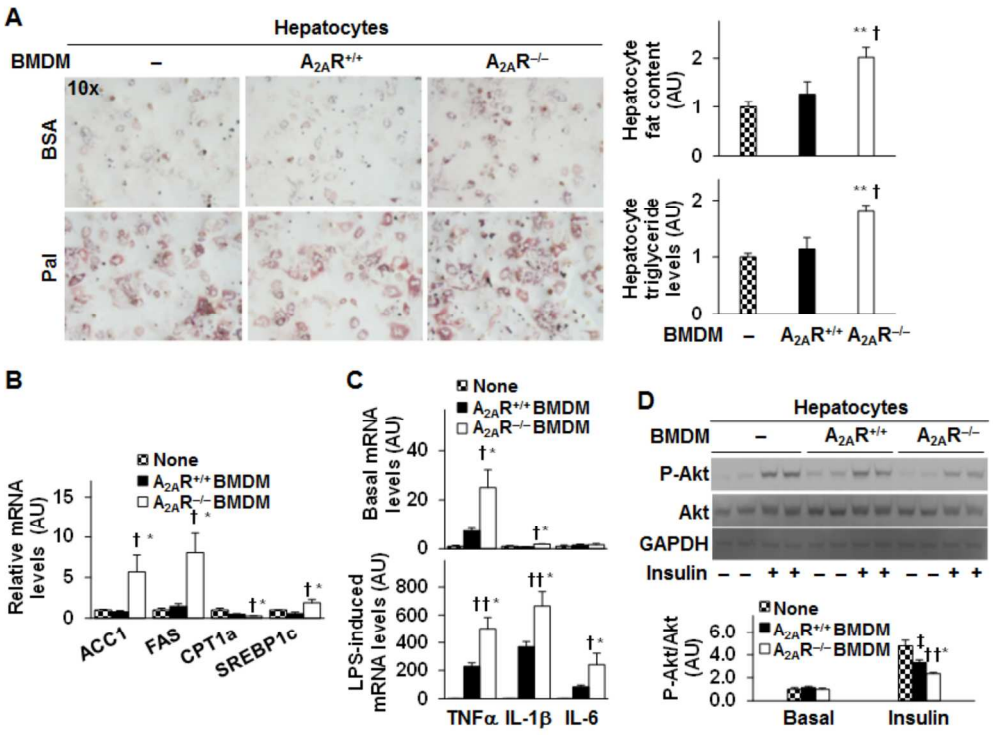

Fig. 5

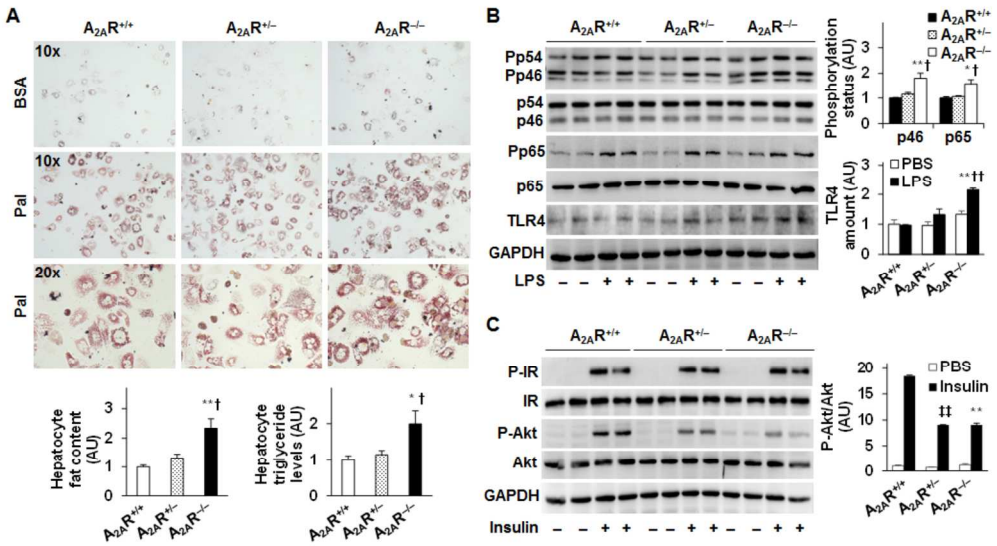

Fig. 6

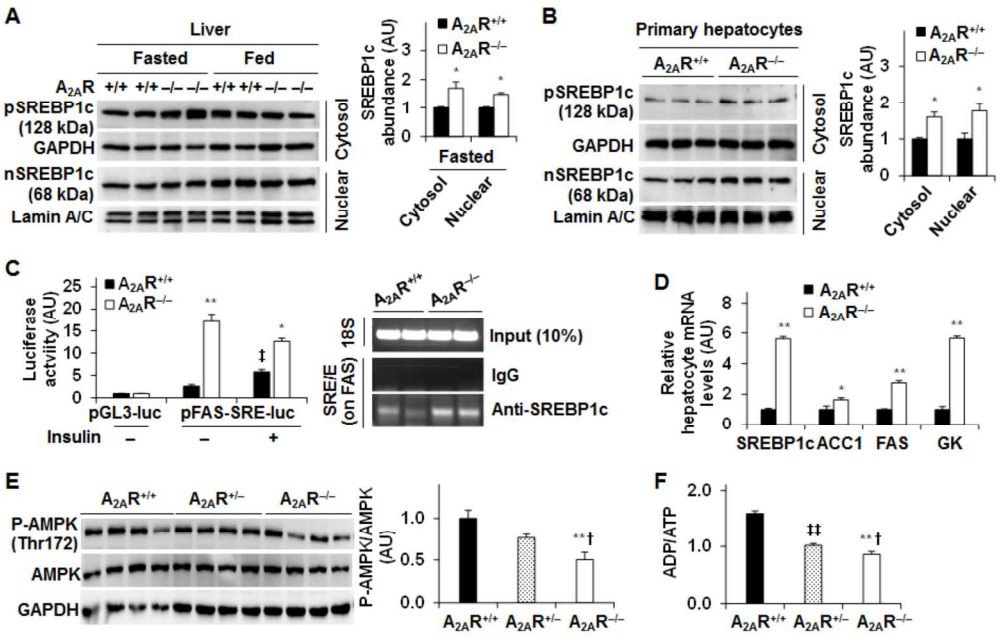

Fig. 7